REQUIREMENTS FOR SUBSCALE SIMULATION OF DELTA-WING VORTEX CHARACTERISTICS

Lars E. Ericsson, Mountain View, California 94040, USA
and
Martin E. Beyers, Institute for Aerospace Research, NRC, Ottawa, Ontario, Canada

Abstract

A review of published experimental results for delta-wing configurations shows that the measured vortex characteristics can differ greatly between the various tests. An analysis reveals that there are two reasons for the observed differences, i.e. 1) dissimilar simulation capabilities, determined by the achievable Reynolds number and the relative severity of the ground facility interference in the test facilities used, and 2) differences in geometric details between the tested models. These factors are usually interconnected as they have their origins in the difficulties in supporting a pure delta wing without essentially changing its geometry, difficulties aggravated by the need for maximizing the model scale to achieve the highest possible test Reynolds number. It is found that modest changes in the model scale and/or test conditions can often reduce these problems to a manageable level.

Nomenclature

b	wing span
c	wing root chord
h	dimensionless wing thickness, = t/c
N	normal force, coefficient C_N = $N/(\rho_\infty U_\infty^2/2)S$
p	static pressure, coefficient C_p = $(p - p_\infty)/(\rho_\infty U_\infty^2/2)$
Re	Reynolds number based upon c and freestream conditions
s	wing semi-span
S	reference area, = projected wing planform area
t	time and wing thickness
U	horizontal velocity
w	width of test section
x	chordwise coordinate
y	spanwise coordinate
z	vertical height above wing plane (Fig. 4)
α	angle of attack, $\dot{\alpha} = \partial\alpha/\partial t$
α_c	pitch-rate-induced camber (Fig. 3)
α_{eff}	effective angle of attack, Eq. (1)
β	angle of sideslip
δ_{LE}	leading-edge bevel angle
Γ	circulation
Λ	leading-edge sweep
ζ	dimensionless z-coordinate, z/c
η	dimensionless y-coordinate, y/s
ξ	dimensionless x-coordinate, x/c
ρ	air density
ϕ	roll angle, $\dot{\phi} = \partial\phi/\partial t$

Subscripts

B	vortex breakdown
c	camber
eff	effective
LE	leading edge
1,2	numbering subscripts
∞	freestream conditions

1 Introduction

According to Maj. Gen. Richard L. Engel, Edwards Air Force Base, the demands on non-flight simulation of combat aircraft high-alpha aerodynamics are increasing in a drive to cut development costs. “Today there is an increasing reliance on modeling and simulation (M&S) and ground testing data, later confirmed by data acquired in the air” [1]. Also, the planned future use of Uninhabited Combat Air Vehicles (UCAVs) [2] will place increasing demands on the simulation of combat aerodynamics in subscale tests, as no extensive effort will be spent on the airframe design [3]. Stealth will be one important design consideration, leading to sharp-edged, tailless air vehicle geometries, employing swept leading and trailing edges. As the UCAVs do not have to be flown much in peace-time, according to USAF Col. M. S. Francis [4], the combat aerodynamics will to an increased extent be determined in subscale tests.

In view of these changes in the aircraft design process it is appropriate to assess present capabilities for simulation of combat aircraft aerodynamics in subscale wind tunnel tests at medium to high angles of attack. To simplify the study of vortical flows characteristic of combat aircraft the basic delta wing has been a popular choice for generic model. Unfortunately, the ability to measure the true delta-wing vortex characteristics has been quite elusive. Recognizing the lack of capability to simulate present and future combat aircraft and UCAVs at full-scale flight conditions, the impact of factors influencing unsteady crossflow characteristics of delta wing planforms in experimental facilities are analyzed in an effort to define important relationships.

2 Subscale Simulation Requirements

There are two performance parameters of a test facility that determine its capability to simulate full-scale aerodynamics using subscale models, i.e., the Reynolds number range and the limitations imposed by ground facility interference.

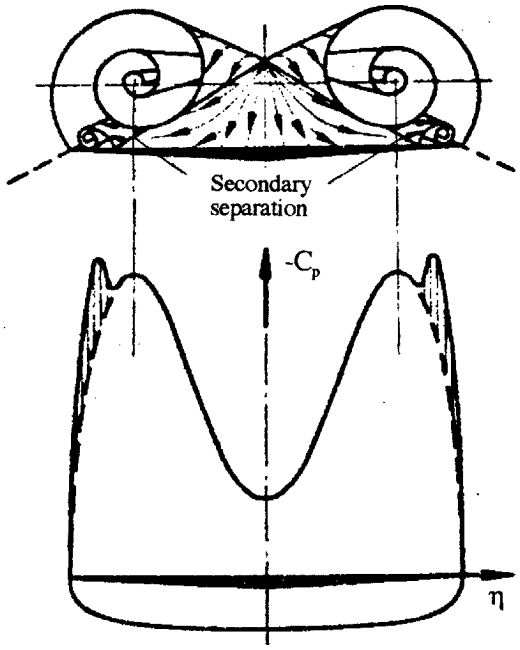

Fig. 1. Effect of secondary flow separation on spanwise pressure distributions on a sharp-edged delta wing [5]

2.1 Reynolds Number Effects

Although it is true that the primary flow separation is fixed by the sharp leading edge of the delta wing, the secondary flow separation is influenced decisively by the Reynolds number of the reattaching flow generated by the primary vortex [5] (Fig. 1). Thus, both the spanwise and chordwise aerodynamic loading will be strongly dependent on Reynolds number, indicating that the subscale simulation difficulties are of concern already in static tests. In dynamic tests the problem is amplified greatly. For example, in the case of a pitching delta wing, the pitch-rate-induced camber effect (Fig. 3) has been shown to have a large influence on the delta wing aerodynamics [6,7], as indicated by the effect of static camber on the vortex-induced loads on a 70 deg delta wing [8] (Fig. 4). The positive camber (illustrated by ζ_o = - 0.0262 in Fig. 4) would be generated during the upstroke of the pitching delta wing (Fig. 3). The camber generates an accelerated flow field over the top surface of the wing. Based upon the observed accelerated flow effect on the boundary layer transition on pitching airfoils and bodies of revolution [9-11],

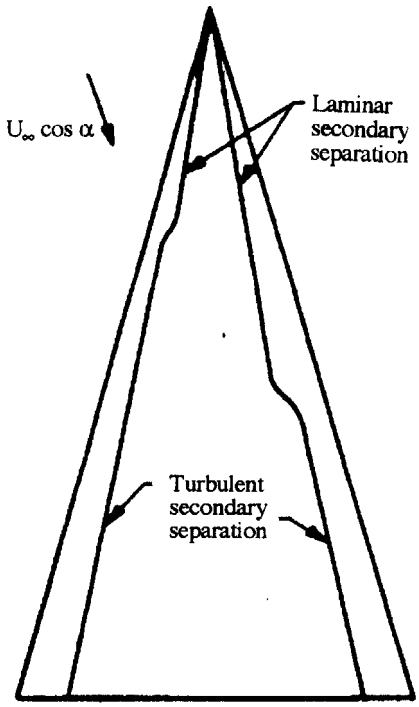

Fig. 2. Effect of sideslip on secondary flow separation [5].

one expects the transition to turbulent flow to be delayed during the upstroke and promoted during the downstroke. This adds an unsteady aerodynamic component to the scaling problem illustrated in Figs. 1 and 2.

One notices that for the investigation of the static camber effect (Fig. 4), Lambourne et al [8] applied distributed roughness to the wing surface close to the apex. At Re = 5.11 x 10^6 it apparently prevented the accelerated flow effect for ζ = -0.026 from changing the flow conditions from turbulent to laminar (Fig. 4) at the apex deflection used. However, it reinforced the decelerated flow effect produced by the negative camber at ζ = 0.026, generating flow conditions that were closer to fully turbulent than for ζ = -0.026, and resulting in a higher than expected suction peak. This explains why the decelerated flow effect for ζ = 0.026 did not, as would be expected, produce a larger decrease of the suction peak than the increase produced by the accelerated flow effect. Instead, it had a lesser effect. The serious implication for dynamic tests with a pitching delta wing model is that the

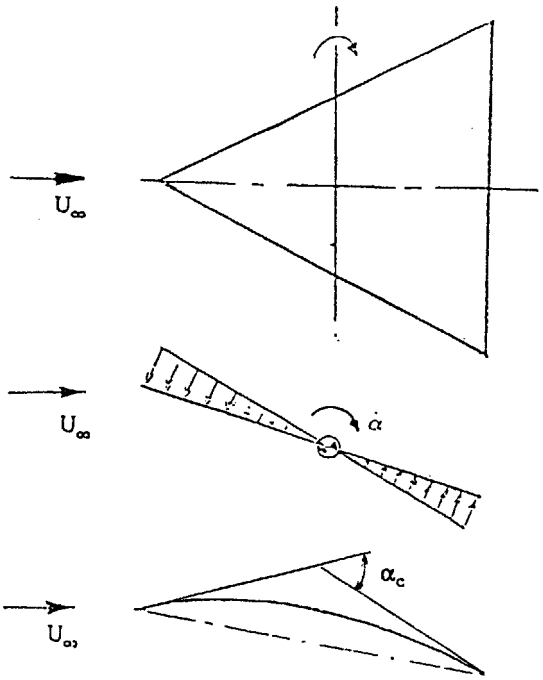

Fig. 3. Pitch-rate-induced camber effect [6,7].

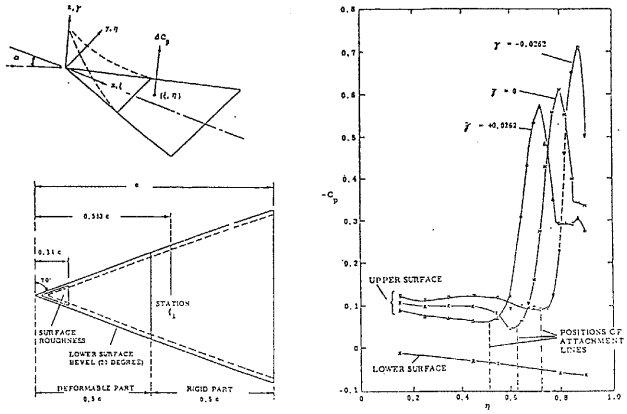

Fig. 4. Spanwise pressure distribution at ξ_1 = 0.583 for deformed 70 deg delta wing at Re = 5.11 x 10^6 and α = 5 deg [8].

distributed roughness used would have given distorted experimental results even at as high a Reynolds number as Re = 5.11 x 10^6. At a lower Reynolds number, such as Re = 2.56 x 10^6 (Ref. 8 and Fig. 5), the distorting effect of the distributed roughness is more severe. Instead of giving increased suction, the positive camber ζ_o = -0.026 actually decreased the suction peak. Such a reversal of flow separation characteristics often occurs when the accelerated flow affects separation via its effect on boundary layer

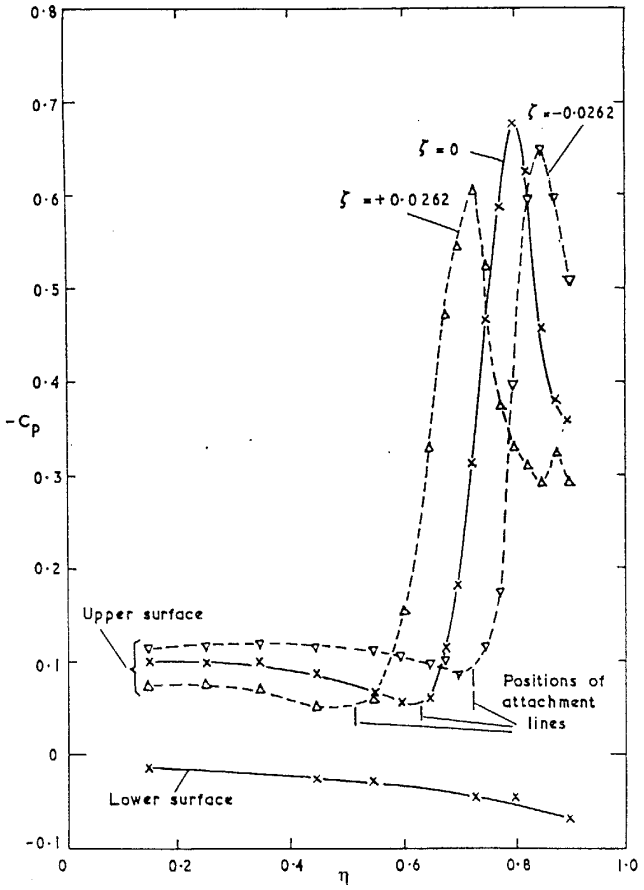

Fig. 5. Spanwise pressure distribution at ξ_1 = 0.583 for deformed 70 deg delta wing at Re = 2.56 x 10^6 and α = 5 deg [8].

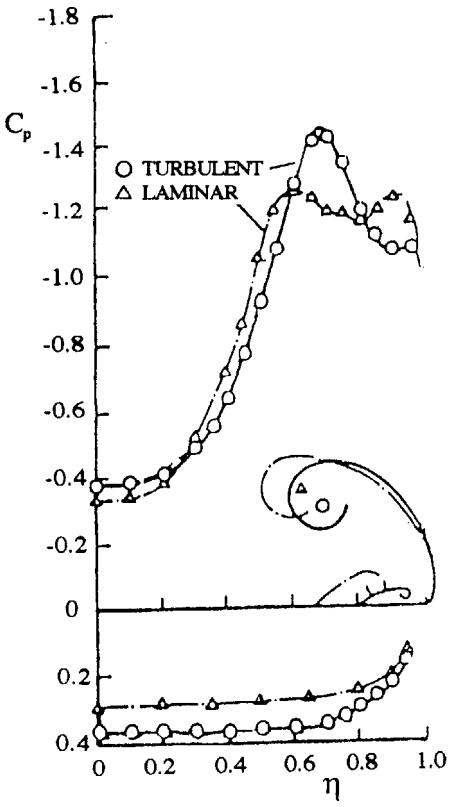

Fig. 6. Spanwise pressure distributions on 70° delta wing for laminar and turbulent flow conditions [5].

transition [9-11]. Apparently, the Reynolds number Re = 2.56 x 10^6 (Fig. 5) was low enough to permit the accelerated flow effect, generated by the negative deflection ζ_o = -0.026, to eliminate transition, thereby converting the secondary flow separation from turbulent to laminar, resulting in the expected decrease of the vortex-induced suction peak [5] (Fig. 6). Thus, dynamic tests at Re = 2.56 x 10^6 would have produced a pitching-induced change of the vortex-induced suction peak with the wrong sign.

At full-scale Reynolds number, when boundary layer transition occurs very close to the apex, the accelerated flow effect on transition acts on a very small region, having an insignificant effect on the overall vortex-induced loads. Thus, if the Reynolds number had been increased from Re = 5.11 x 10^6 to Re > 10^7, the distributed roughness near the apex would probably have produced vortex-induced loads close to those realized in full-scale flight. However, if this cannot be accomplished, it would be better to perform thedynamic test at laminar flow conditions. Figure 6 demonstrates that the vortex-induced contribution to pitching and rolling moments would be of roughly the same magnitude for laminar as for turbulent flow conditions [5].

For a rolling delta wing the roll-rate-induced camber [12] (Fig. 7) will have a similar effect on the leading-edge vortices as the pitch-rate-induced camber (Fig. 3). This is confirmed by the tests of a 65 deg delta wing [13], which produced experimental results demonstrating that the roll-rate-induced camber had a powerful effect on the vortex-induced loads. As no attempt was made to trip the boundary layer, the problem discussed above for the pitching delta wing was avoided. As the presence of a centerbody had a very significant effect [12,14], any attempt to simulate full-scale flow conditions by the use of boundary

layer tripping devices on the delta wing and centerbody would be likely to have severely distorted the steady and especially the unsteady aerodynamic measurements.

The problems discussed here for tests with pitching or rolling delta-wing models support the conclusion reached in Ref. 15 that "dynamic simulation of full-scale aerodynamics is only possible when testing at the full-scale Reynolds number." Thus, any attempt to influence boundary layer transition through the application of tripping devices is fraught with difficulties, especially in dynamic tests.

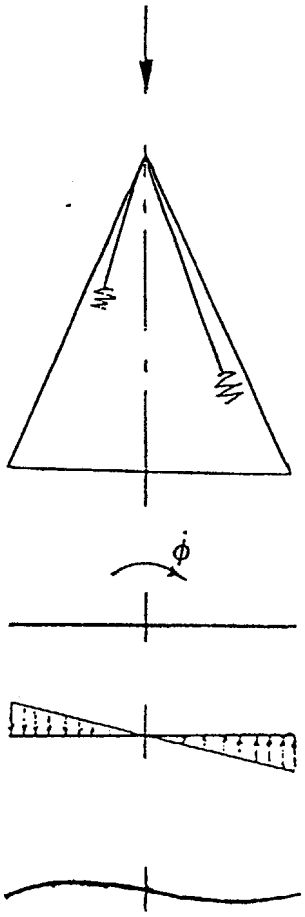

Fig. 7. Roll-rate-induced camber effect [12].

2.1.1 Instrumentation Interference Effects

The experimental results [16] at $\alpha = 30^{o}$ for an $80^{o}/70^{o}$ double-delta wing (Fig. 8) illustrate the simulation problem one faces through unintended effects on the aerodynamic characteristics of intrusive instrumentation. At the test Reynolds number laminar flow conditions existed at 75% chord until a pressure sond was used for off-surface measurements. Its presence caused a transition from laminar to turbulent flow conditions, with associated large changes of the spanwise pressure distribution (Fig. 8). Another situation [8] is illustrated in Fig. 9. The figure shows that the disturbance generated on the bottom, windward side of a 70 deg delta wing by the pressure transducer closest to the leading edge, at station ξ_1, caused the leading-edge vortex to be deflected inboard and a new leading-edge vortex to be initiated at ξ_1.

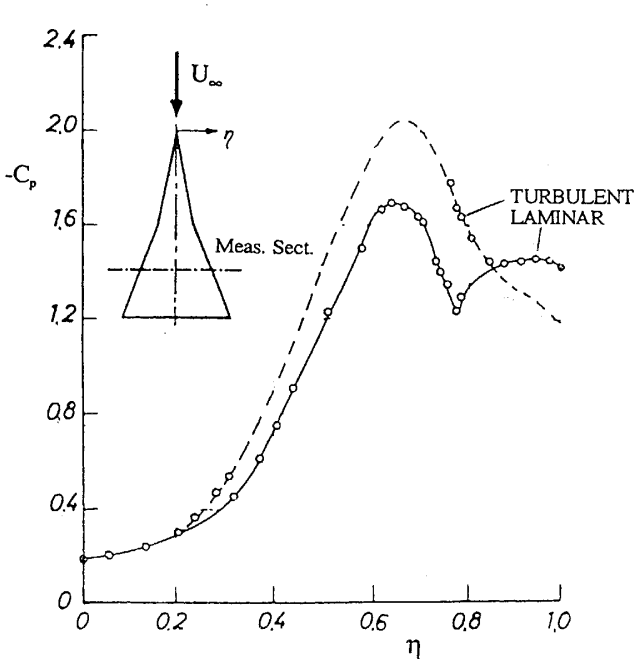

Fig. 8. Effect of total pressure sond on the spanwise pressure distribution at 75 % chord on $80^{o}/70^{o}$ double-delta wing [16].

Another example of the effect of small disturbances on vortical flow has been described by Skow: [17] "… an indentation on one side of the aircraft near the apex of the leading-edge extension (LEX), with a depth of less than 0.10 inch, could cause the aircraft to have very violent departure tendencies at high incidences. A tenth of an inch at airplane scale is rather minute at wind tunnel model scale, so it really makes you wonder whether we can produce reliable, repeatable wind tunnel data." As in the case of distributed roughness, for isolated roughness elements, such as imperfections of the leading

edge, the equivalent knick height would be a function of the local boundary layer thickness and, in particular, the location relative to the transition front [18]. If the tests could be conducted at full-scale Reynolds number in a pressurized facility the concept of an equivalent imperfection height would still be needed for subscale tests since, as in the case of roughness, effective isolated element height does not scale geometrically when boundary layer transition is involved.

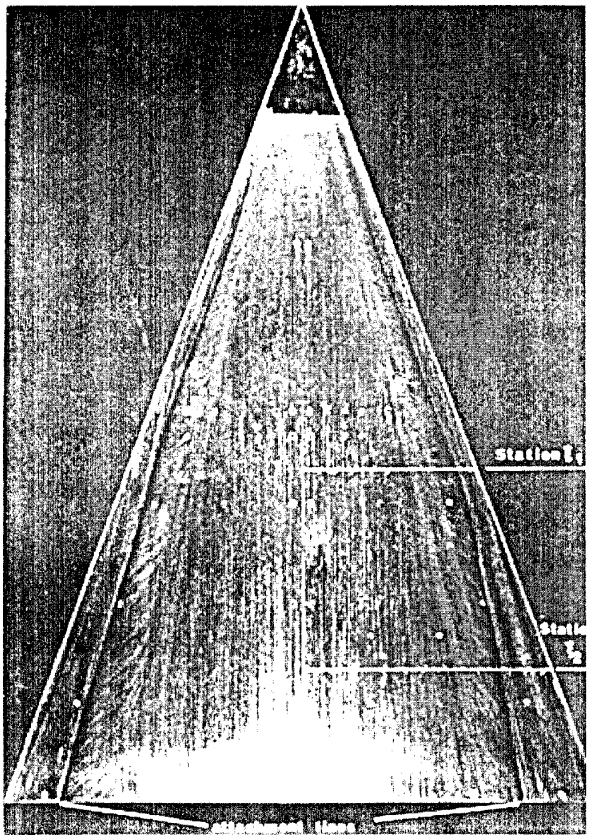

Fig. 9. Effect of pressure-transducer-created windward side microasymmetry at $\xi_1 = 0.583$, $\eta = 0.90$ on leading-edge vortex shedding of a 70 deg delta wing [8].

2.2 Model Geometry Effects

A recent review [19] of experimental results for vortex breakdown on 65 deg delta-wing configurations raises many questions that need to be answered [20]. The huge differences between empirical predictions [21,22] (Fig. 10) reflect the differences observed between existing experimental results. A 65 deg delta-wing-body model (Fig. 11) was tested extensively, giving the results [21,23-25] shown in Fig. 12. Although the model was supposedly the same, the experimental results fall in two groupings, those of Ref. 21 versus those presented in Refs. 23-25. One prominent distinction is that one set [21] is for turbulent flow conditions (Re = 3.6 $\times 10^6$) whereas the other set [23-25] is for laminar flow conditions (Re $\times 10^{-6}$ = 0.10, 0.29, and 0.32).

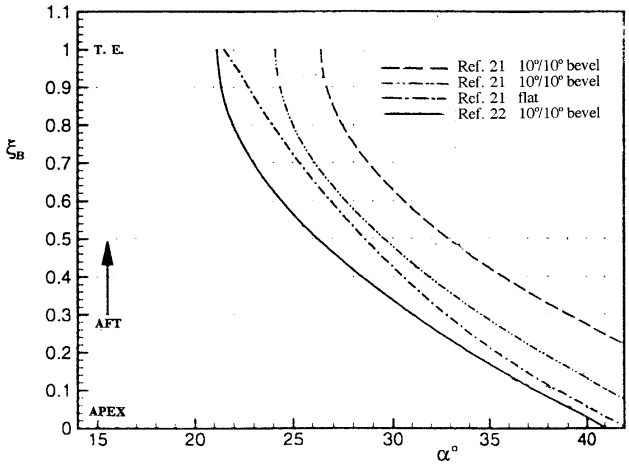

Fig. 10. Empirical prediction of vortex breakdown on 65 deg delta-wing configurations.

Although in the tests reported in Refs. 23 and 24 the centerbody geometry was slightly different from that tested in Refs. 21 and 22, the differences are small, and the different flow conditions, laminar versus turbulent, probably had the largest effect. This is confirmed by the comparison made in Fig. 13 between laminar water tunnel tests at Re = 0.015 $\times 10^6$ (Ref. 26) and turbulent wind tunnel tests [21] at Re = 3.6 $\times 10^6$, demonstrating that the effect of Reynolds number can be large. In Ref. 28 the turbulent experimental results [24] for the delta-wing-body configuration (Fig. 11) were compared with the turbulent measurements of vortex breakdown on pure 65 deg delta wings. The results, shown in Figs. 14a and 14b, demonstrate that the effect the centerbody is large [14]. In the tests of the 65 deg delta-wing-body configuration [21] (Fig. 11) the vortex breakdown location varied with alpha as shown in Fig. 14a, occurring significantly aft of the location measured by others [27-29] for a pure 65 deg delta wing.

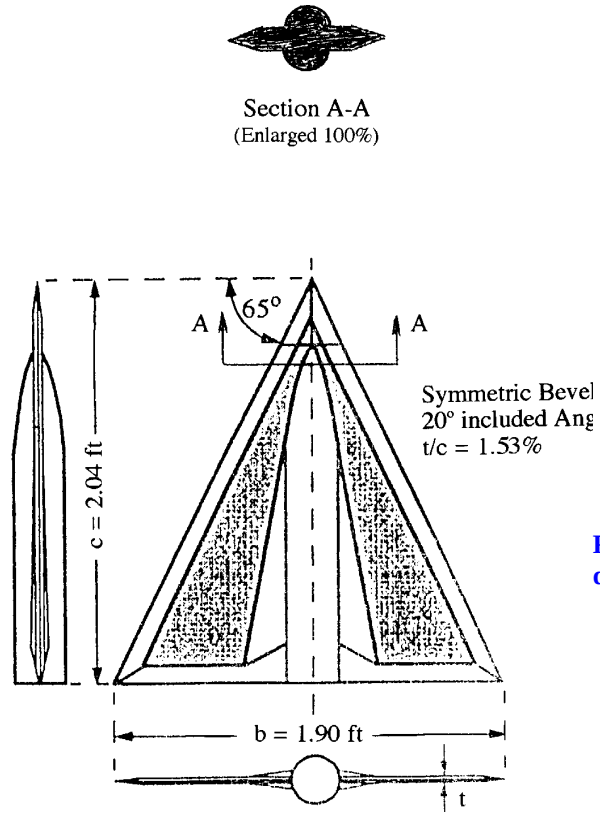

Fig. 11. Test model of 65 deg delta-wing-body configuration ($\delta_{LE} = 10^o$) [21].

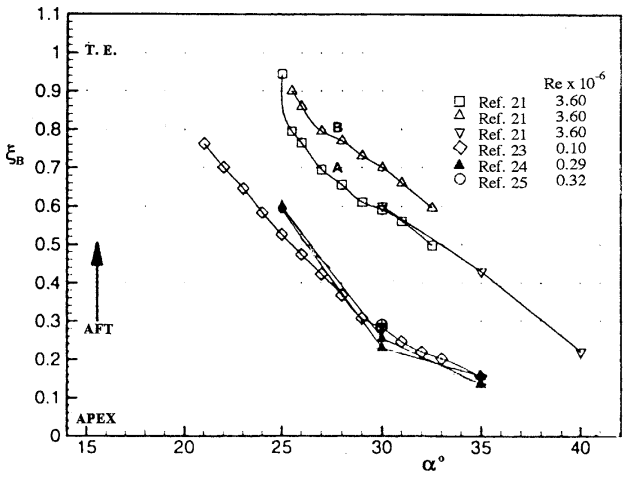

Fig. 12. Measured vortex brekdown location on 65 deg delta-wing-body configuration.

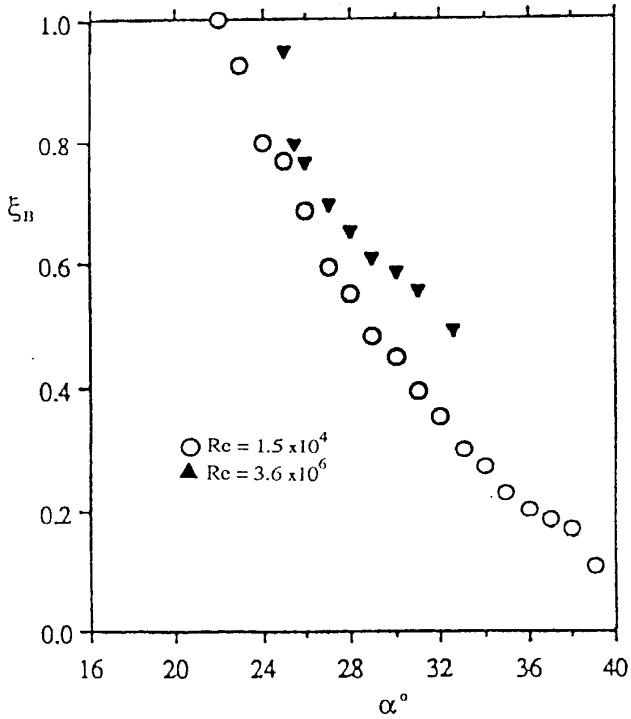

Fig. 13. Effect of Reynolds number on the influence of a centerbody on the breakdown location of a 65 deg delta wing measured in a laminar water tunnel test [26] compared with turbulent wind tunnel test results [21].

The angle of attack for the data in Fig. 14a needs to be corrected for the effect of the leeside bevel angle δ_{LE} at the leading-edge [30]. The effective angle of attack is

$$\alpha_{eff} = \alpha - \tan^{-1}(\tan \delta_{LE} \cos \Lambda) \qquad (1)$$

When the test results in Fig. 14a are plotted against the effective angle of attack α_{eff}, corrected for the effect of δ_{LE}, 7.5° for W&K [29] and 10° for H&H [21], it becomes evident that the fuselage had a large effect on vortex breakdown in the H&H test (Fig. 14b). The L&B data [27,28] have not been corrected. Together with the large bevel angle $\delta_{LE} = 16^o$ one also has to consider that this wing was seven (7) times thicker than the others. As is pointed out in Ref. 27, the all important apex flow conditions are very sensitive to wing thickness, a dependence which in turn is affected by the edge geometry [30]. At $\alpha_{eff} = 30^o$ the breakdown on the delta-wing-body configuration [21] (Fig. 11) occurs more than 30% chord aft of the breakdown location for a pure delta wing [27-29] (Fig. 14b). How the observed delay of vortex breakdown can be generated by the body-induced camber effect is described in Ref. 14.

The experimental results [23,26-28,31-33] in Fig. 15 for a pure 65 deg delta wing show that

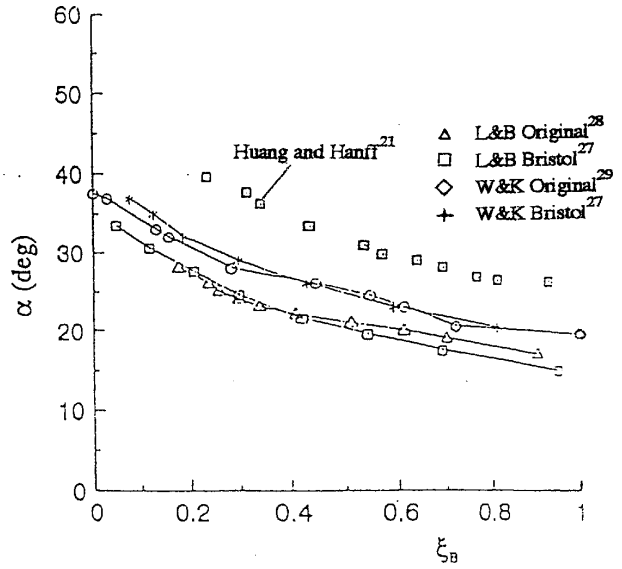

a. Original test results.

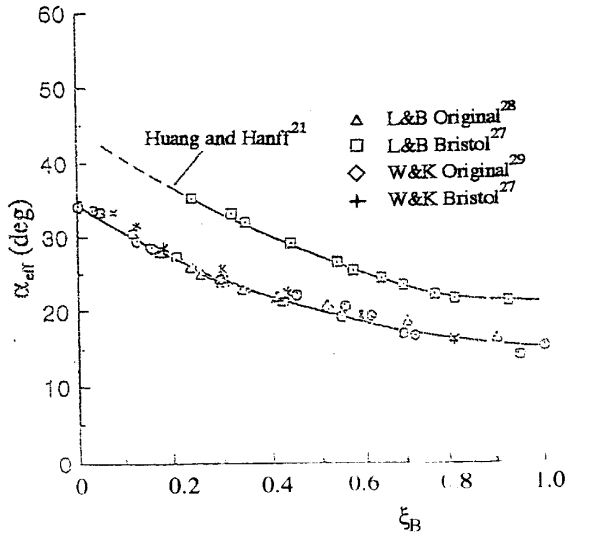

b. Test results corrected for the effect of leading-edge bevel angle.

Fig. 14. Measured breakdown location $\xi_B = f(\alpha)$ of a 65 deg delta wing with and without centerbody.

the bevel angle on the lower side had no significant effect on the breakdown location. It appears to have been determined solely by the Reynolds number, Re > 0.2 x10^6 producing breakdown at a location $\Delta\xi_B \approx 0.2$ forward of that measured at Re ≤ 0.1 x10^6. This is in agreement with the conclusion drawn from experiments with double-delta wings: [34] "The vortex breakdown location is characterized by a forward movement toward the apex of the model as the flow Reynolds number is increased." The body-on results in Fig. 12 showed the opposite data trend, with breakdown occurring $\Delta\xi_{VB} \approx 0.3$ farther aft at Re = 3.6 x10^6 than at Re ≤ 0.29 x10^6. Obviously, the viscous flow effects are influenced greatly by the presence of the centerbody. A reexamination of the effect of a centerbody or fuselage on delta wing vortex breakdown [35] should provide an explanation of the opposite Reynolds number effects for body-on (Fig. 12) and body-off delta-wing configurations (Fig. 15). The experimental results by Panton [36], which were included in Fig. 4 of Ref. 19, have been excluded based upon the following comment in Ref. 36: "At high angles of attack, wall interference effects were likely so increments between configurations are more significant than absolute levels."

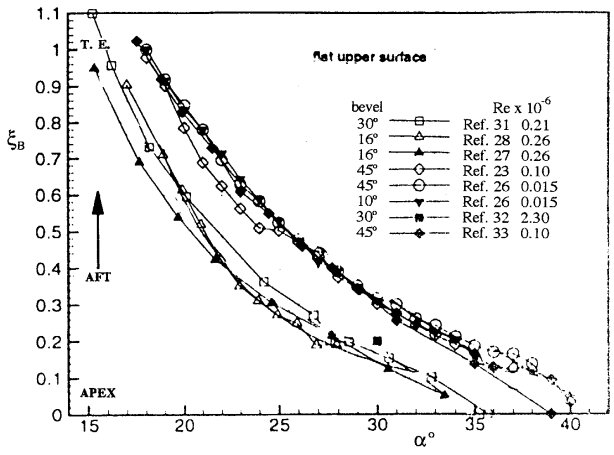

Fig. 15. Effect of Reynolds number on vortex-breakdown location $\xi_B = f(\alpha)$ for a pure 65 deg delta wing with flat upper surface.

2.2.1 Effect of Centerbody

In contrast to the results in Fig. 12, the body geometry used on a 69.33° delta wing promoted vortex breakdown [37] (Fig. 16). In that case the body induced a negative camber effect [14,15], which has been shown to promote vortex breakdown [28] (Fig. 17b). If the center-body in Fig. 16 is moved aft, the situation shown in Fig. 11 results. In that case the camber effect generated by the slender forebody is of the opposite, positive type [38], which has been

shown to delay breakdown [28] (Fig. 17a). A case in between is represented by the centerbody used by Guglieri and Quagliotti [31] (Fig. 18), which promoted vortex breakdown. The bluff nose did apparently not noticeably moderate the negative camber effect generated by the cylindrical afterbody [37] (Fig. 16).

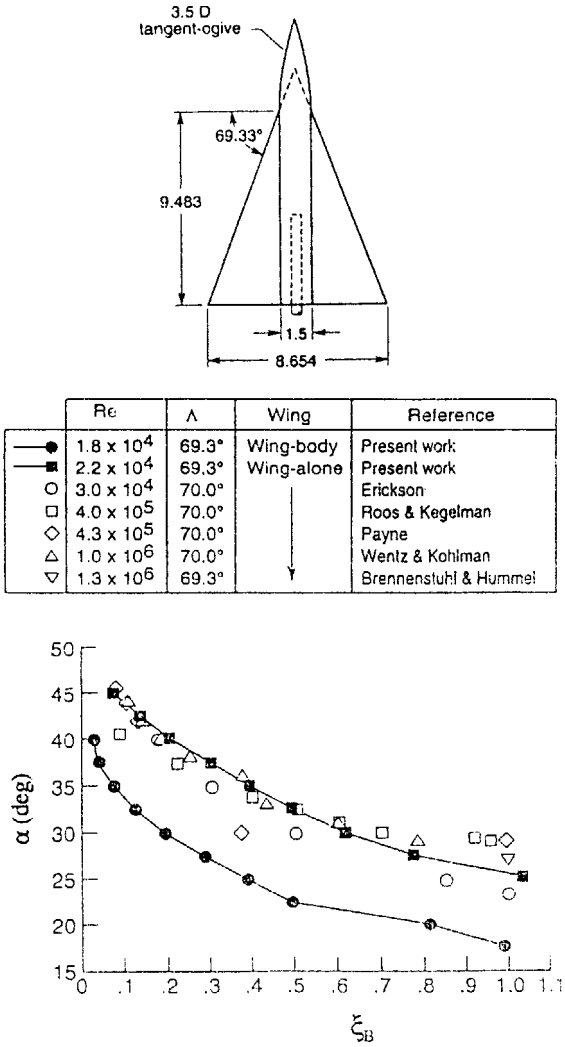

Fig. 16. Effect of cylindrical centerbody on $\xi_B = f(\alpha)$ for a 69.3 deg delta wing [37].

Going back to Figs. 11 and 12, one can visualize how the viscous flow had a bluntening effect on the centerbody, which for the laminar flow conditions existing at low Reynolds number could be large enough to change the effective body geometry towards that in Fig. 18. Thus, at Re = 0.015 x10^6 (Ref. 26 and Fig. 19) the forebody-induced positive camber effect,

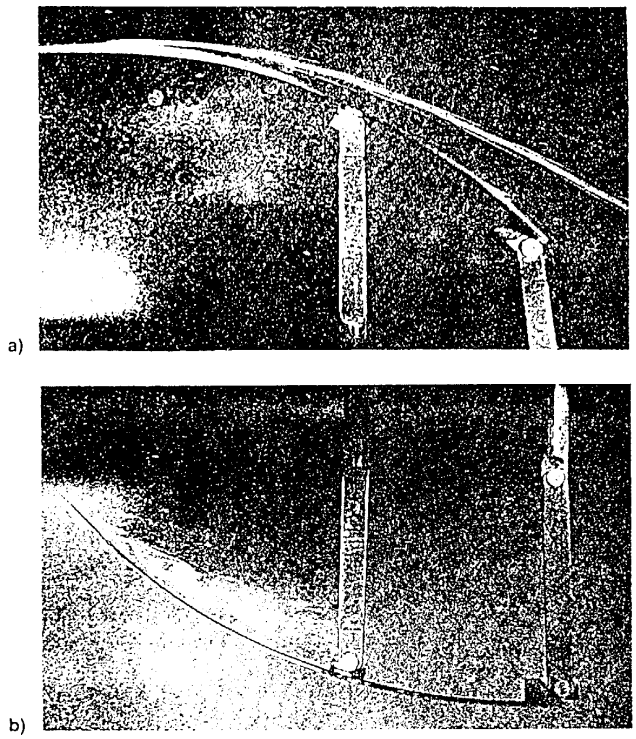

Fig. 17. Effect of a) positive and b) negative longitudinal camber on the vortex breakdown of an 80 deg delta wing [28].

observed at Re ≥ 1.0 x10^6 (Figs. 12-14), was nullified. Such a large difference in viscous flow effects is not unexpected, considering that the ratio between boundary layer thickness and bevel width was 15 times larger in the water tunnel test [26] (Fig. 19) than in the wind tunnel experiment [21] (Fig. 14), according to a statement made in Ref. 26. The lost effect of the centerbody on the position of the leading-edge vortex in the water tunnel [26] (Fig. 19) is further evidence of the large boundary-layer-displacement effect. In Fig. 20 an attempt has been made [38] to illustrate how this "viscous fairing" could have had a negligible influence on the effective model shape in the turbulent wind tunnel test (Fig. 20a), whereas it was likely to have changed completely the effective geometry in the water tunnel test (Fig. 20b). The increased bluntness generated by the "viscous fairing" caused the centerbody on the water tunnel model to act somewhat like the one in Fig. 18, completely eliminating the forebody-induced positive camber effect existing for the negligible "viscous fairing" present in the wind tunnel test (Fig. 20a).

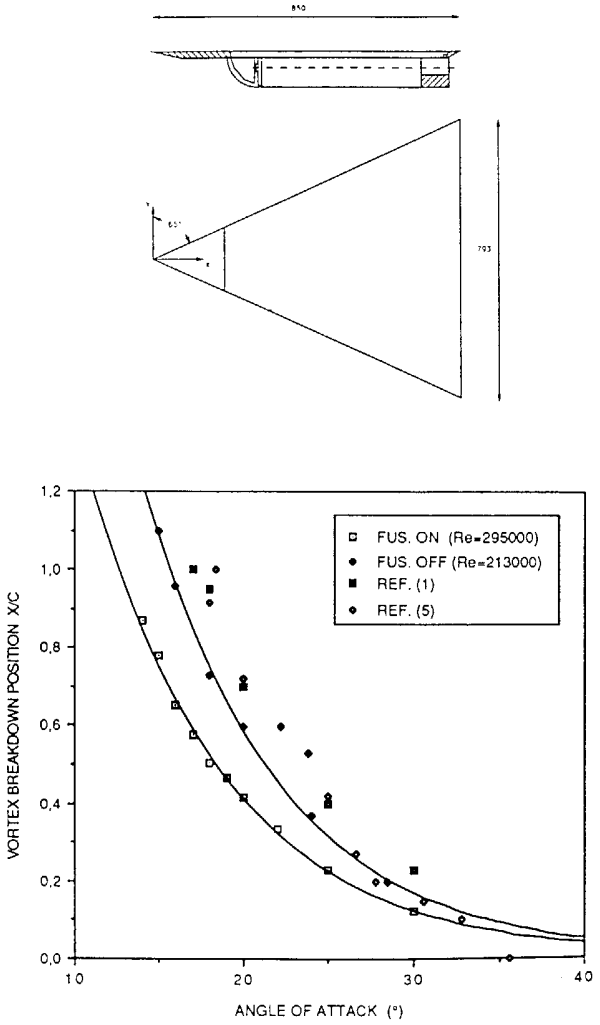

Fig. 18. Effect of hemisphere-cylinder centerbody on the vortex-breakdown location $\xi_B = f(\alpha)$ for a 65 deg delta wing [31].

A similar "viscous-fairing" effect was observed in water tunnel tests at Re = 0.015 x10^6 of a pure 65 deg delta wing (Fig. 21) [26]. The experimental results show how the influence of the 10 deg leading-edge bevel angle was strongly affected by the wing thickness. For the 0.8% thick wing the "viscous fairing" suppressed totally the effect of $\delta_{LE} = 10^o$. Increasing the wing thickness to 1.6% and finally to 7.5 % gradually increased the effectiveness to the expected value, $\alpha_{eff} = 4.3^o$, given by Eq. (1).

In principle one must agree with the conclusion drawn in Ref. 19: "The sensitivity of

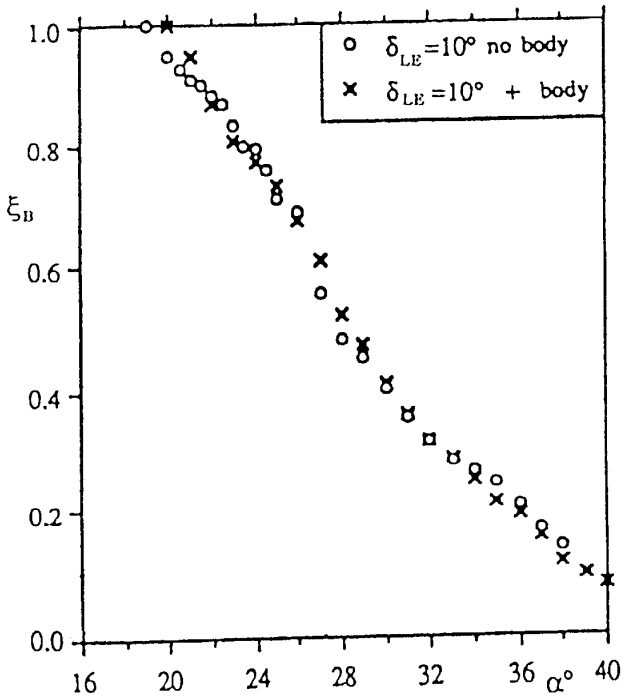

Fig. 19. Measured negligible effect of centerbody on the vortex breakdown of a 65 deg delta wing at laminar flow conditions, Re = 0.015 x 10^6 (Ref. 26).

the flow to small geometric changes suggests that an efficient means of flow control is possible." However, the experimental and theoretical results in Ref. 19 also demonstrated that further research is needed before the flow physics will be understood to the degree needed for the development of "micro-means" for delta-wing flow control, research that by necessity will include the interactive use of experiment and CFD, with careful attention to the inherent inaccuracies of both investigative methods.

In addition to the discussed problem of Reynolds number scaling in experimental investigations one must also consider ground facility interference effects [39,40]. As they usually are rather difficult to determine and correct for after the tests have been performed, they should be considered when planning the tests, at which time modest changes in model size and/or model support structure often can bring the impact of ground facility interference on data accuracy down to a tolerable magnitude.

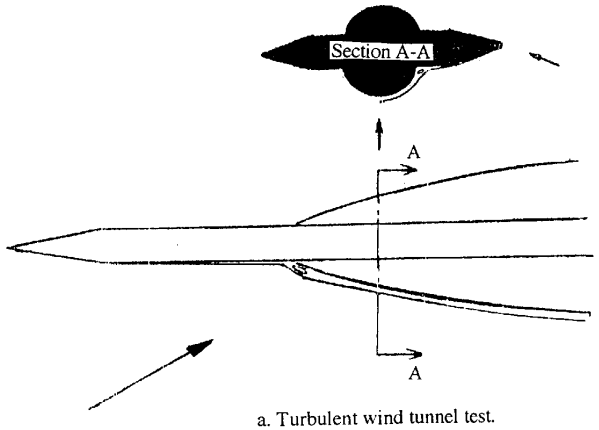

a. Turbulent wind tunnel test.

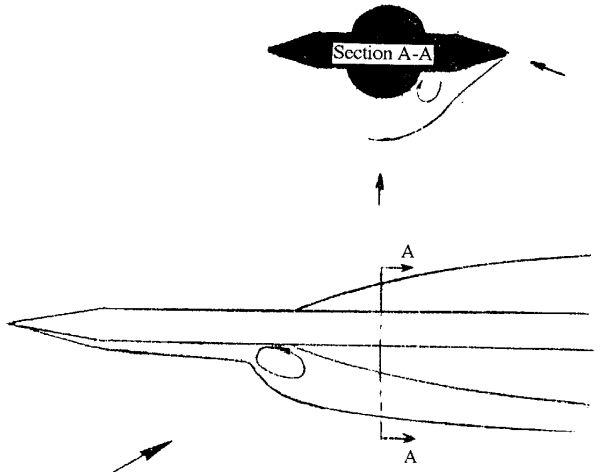

b. Laminar water tunnel test.

Fig. 20. Conceptual "viscous fairing" effects on 65 deg delta-wing-body configuration [38].

2.3 Ground Facility Interference

Ground facility interference comprises two equally important components, i.e., support interference and wall interference. An analysis of recently published experimental results reveals that this fact has often been overlooked. For instance, the difference between test results for differently sized models of otherwise equivalent delta wing geometries is often ascribed exclusively to one of the two components, e.g., wall interference, as will be discussed in what follows.

A recent review and further analysis of factors influencing the vortex breakdown measured on delta wings [41] reveals

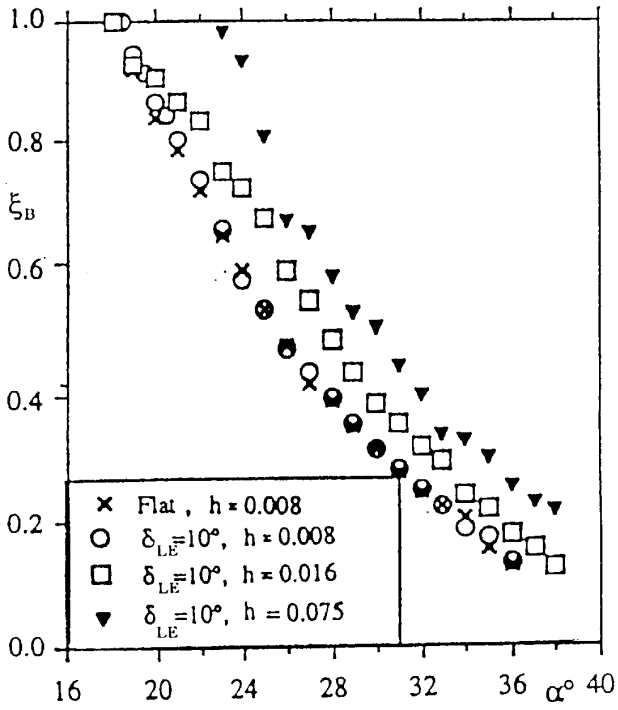

Fig. 21. Influence of wing thickness on the effect of leading-edge bevel δ_{LE} = 10° in water tunnel test of a pure 65 deg delta wing [26].

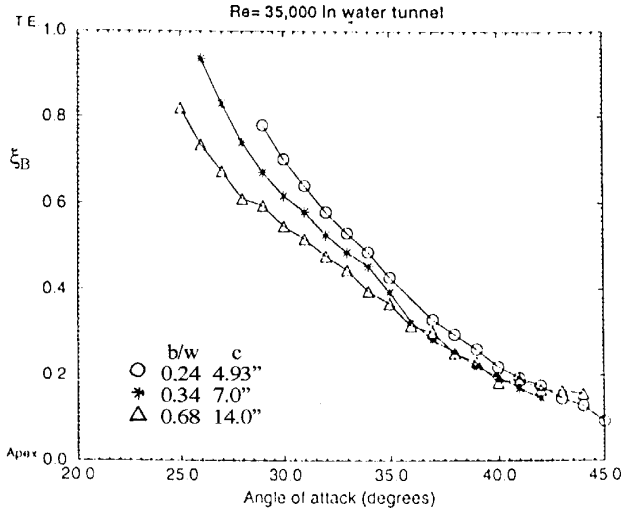

Fig. 22. Effect of model size on vortex breakdown of 70 deg delta wing [41].

inconsistencies, which could have been introduced by the presence of both components of ground facility interference. The results of these experiments and associated analysis [41] appear to contradict the conclusions drawn from an earlier analysis [39]. This illustrates the complexity of the facility interference problem. The earlier analysis [39] was updated [42] by

analyzing the inconsistencies described in Ref. 41.Figure 22 shows that increasing the size of the 70 deg delta wing model caused the vortex breakdown to occur closer to the apex [41]. This data trend, obtained in water tunnel tests at Re = 35,000, is opposite to that obtained in wind tunnel tests [43] (Fig. 23). The general data trend in the latter results can be explained by the longitudinal wing camber generated by the wall-induced upwash along the leading edge of the delta wing [39,40,43]. The results in Fig. 22 were explained in Ref. 41 by the wall-induced upwash effect, represented by the resulting change of the effective angle of attack at the wing center of

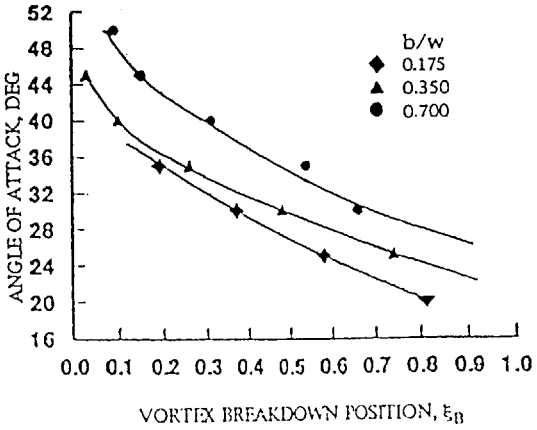

Fig. 23. Wind tunnel wall interference effects on the vortex breakdown of a 70 deg delta wing [43].

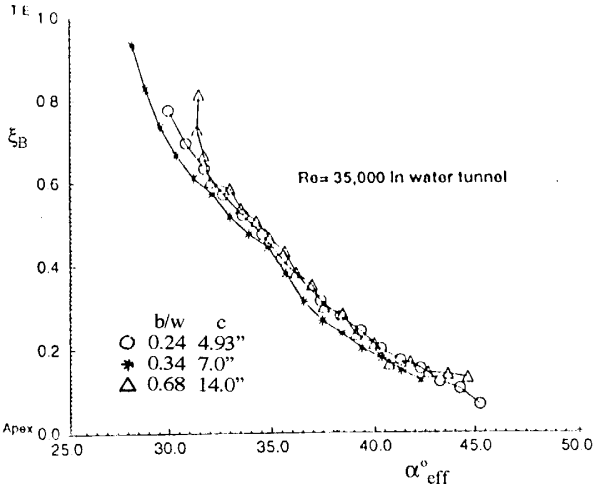

Fig.24. Effect of model size on the vortex breakdown of a 70 deg delta wing as a function of effective angle of attack [41].

pressure. When correcting the measurements (Fig. 22) for this alpha effect the results regrouped as shown in Fig. 24. Although the spread between the curves is decreased in Fig. 24 compared to Fig. 22, the conclusion drawn [41] that "the curves collapse rather well" is not well founded. For some reason the data for the mid-sized model (c = 7"), which fell midway between the original, uncorrected curves in Fig. 22, falls outside of the "collapsed" curves for the smaller (c = 4.93") and larger size (c = 14") models in Fig. 24.

It is well established that vortex breakdown moves towards the apex with increasing angle of attack [29], as illustrated by Figs. 22 and 23. Consequently, the wall-induced increase of the effective angle of attack should have promoted breakdown, as stated in Ref. 41. However, experimental results of the effect of camber on the vortex breakdown of an 80 deg delta-wing [28] (Fig. 17) indicate that the wall-induced camber effect [39,43] should dominate over the effect of the increase of the mean angle of attack [41]. In the case of the positive camber (Fig. 17a), the effective angle of attack at the wing center of pressure is large compared to that for negative camber (Fig. 17b). Still, vortex breakdown occurs downstream of the trailing edge in the former case (Fig. 17a), in sharp contrast to the occurrence of breakdown close to the apex for the case of negative camber, in spite of the lower effective angle of attack over the central wing area (Fig. 17b). Thus, one can definitely not neglect the wall-induced camber effect, as is done in Ref. 41. However, from Fig. 17 it would appear to be justified to neglect the wall-induced change of the effective, mean angle of attack, the only effect considered in Ref. 41. The theoretical basis for this is as follows.

2.3.1 Effects of Induced Camber

The delta wing analysis in Ref. 44, which utilizes Polhamus' leading-edge-suction analogy [45], shows that the vortex lift is solely determined by the local crossflow conditions at the leading edge. In contrast, the loads on the inboard portion of the wing are not solely dependent upon the local, effective angle of attack but are also

influenced by the flow conditions at the leading edge through the flow entrainment action of the leading-edge vortices (Fig. 25).

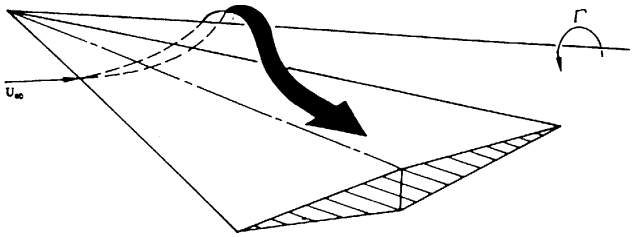

Fig. 25. Entrainment effect of the leading edge vortex [44].

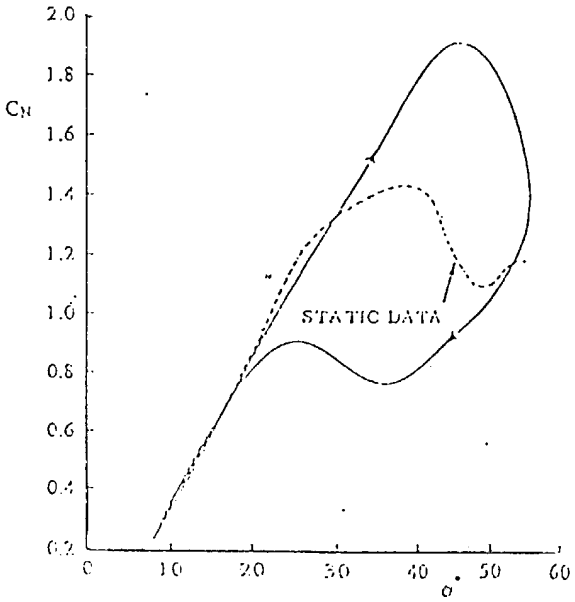

Fig. 26. Dynamic $C_N(\alpha)$ characteristics of a pitching, sharp-edged 70 deg delta wing [49].

Additionally, it was shown in Ref. 46 that the effect of sideslip on the vortex lift was determined satisfactorily by only considering the local flow conditions at the leading edge. This was also found to be the case for the determination of the effect of roll angle and roll rate on the vortex-induced lift and associated rolling moment [47]. It is, therefore, no surprise to find that the local flow conditions at the leading edge are completely dominant over the flow conditions existing over the inner wing when determining the location of vortex breakdown [28] (Fig. 17). The same is, of course, also true when considering the relative effects of the pitch-rate-induced camber α_c (Fig. 3) and the effective, mean angle of attack [48]. The large overshoot of static C_{Nmax} , observed during the upstroke for a pitching delta wing [49] (Fig. 26), is mainly a result of the pitch-rate-induced positive camber. The negative camber generated during the downstroke promotes breakdown, resulting in the measured large undershoot of static C_{Nmax}, all in agreement with the observed effects of camber on static vortex breakdown [28] (Fig. 17).

Thus, the data trend in Fig. 22 cannot be explained through representing the wall interference by the upwash induced at the wing center of pressure, as suggested in Ref. 41. It must be a result of other important components of ground facility interference [39], i.e., other manifestations of wall interference [50], or of support interference [51,52], which in high-alpha tests often is of more concern than the wall interference.

2.3.2 Coupled Support/Wall Interference

Unfortunately, there is no useful information in Ref. 41 about the support structure used. Until such information becomes available one is forced to speculate. It is reasonable to assume that the same support structure was used for the three models. It was demonstrated by Hummel [53] that an obstacle placed one chord length downstream of the trailing edge of the delta wing caused vortex breakdown to move from a position downstream of the trailing edge to roughly midchord (Fig. 27). It has also been shown that the sting-strut support structure used in high-alpha tests has a similar effect, greatly promoting vortex breakdown on a delta-wing model [50,51]. If the sting- strut support structure was one chord length downstream of the trailing edge of the large model (c = 14” in Fig. 22), one would expect, based on Fig. 27, that vortex breakdown would have been promoted to occur farther forward of the trailing edge than in the absence of the support structure. In the case of the smaller models (c = 7” and c = 4.93” in Fig. 22) the sting-strut juncture would have been respectively 2 and 2.85 chord lengths

downstream of the trailing edge, causing progressively less promotion of vortex breakdown, all in agreement with the test results in Fig. 22.

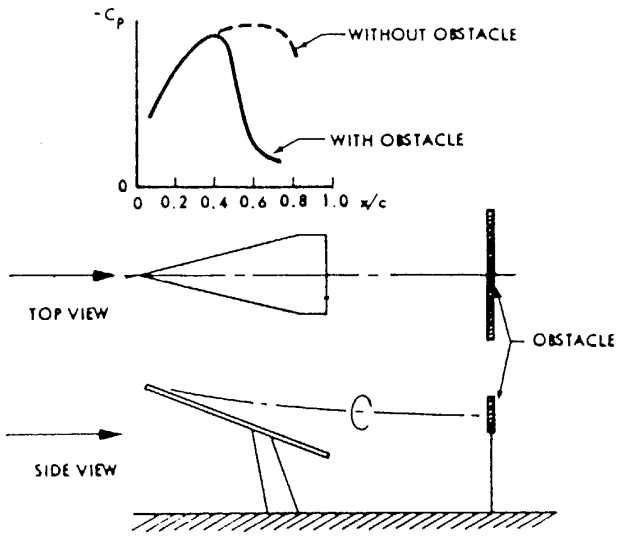

Fig. 27. Promotion of vortex breakdown on a 75 deg delta wing caused by a downstream obstacle [53].

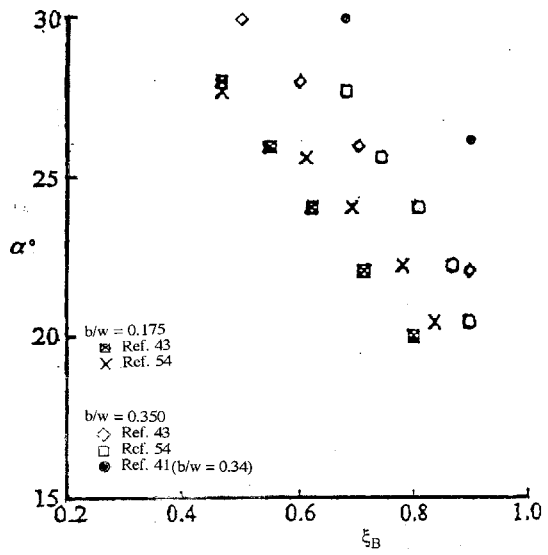

Fig. 28. Comparison of vortex breakdown on 70 deg delta wing measured in different test facilities.

The effect of model size on the location of vortex breakdown has been measured in a more recent investigation [54]. The results shown in Fig. 28 were obtained for a 70 deg delta wing. The emphasis in Ref. 54 was on the effect of wall interference and, as in Ref. 41, no information was given about the support structure. The comparison in Fig. 28 with Weinberg's results [43] shows relatively good agreement, especially for b/w = 0.35. When including the results for b/w = 0.34 from Ref. 41, the situation becomes more complicated. If the support structure used in Ref. 54 was similar to that in Ref. 43, and assuming as before that the support interference in Ref. 41 was small for b/w = 0.34 (and b/w = 0.24), the results in Fig. 28 would indicate that for b/w = 0.35 support interference caused vortex breakdown in Refs. 43 and 45 to occur 20% of chord upstream of that observed in Ref. 41. Decreasing the model size to b/w = 0.175 should have increased the distance from the model to the support structure sufficiently to cause the support interference to possibly become of negligible magnitude. Thus, for both b/w = 0.35 and b/w = 0.175 the differences between Refs. 43 and 54 probably fall within the data accuracy in the two facilities. However, for the larger model size, b/w = 0.35, both appear to have had more severe support interference than the Notre Dame facility [41].

Both wall interference and its coupling with support interference are greatly complicated when sideslip in the wing plane is introduced by nonzero β and/or ϕ. In that case the wall-induced effects have a sidewash componenent, interfering with the coupling between the leading-edge vortices and influencing differential vortex breakdown. As a result, when b/w is increased it becomes increasingly difficult to measure the rolling moment accurately [50]. This problem of yaw-roll coupling effects is of even more concern in the case of the unsteady aerodynamics, based on the experience with a 60 deg delta wing at high angles of attack [55,56].

2.3.3 Nonuniform Flow due to Test Installation

When a strut support structure is used the class of interference discussed with reference to Fig. 27 is

generally the most severe [50]. However, when a large model is tested the situation becomes more complex. Vortex breakdown is promoted upstream of the strut flow stagnation region, but delayed in the outer region of the test section characterized by a favorable pressure gradient. Comparing Figs. 22 and 23 it is noticed that the trends in the curves for the two smaller models ($b/w \leq 0.35$) are similar in that the effect of model size becomes negligible at high alpha. However, at $\alpha < 35^o$ the effects are completely the opposite, i.e., increasing b/w from 0.175 to 0.35 in Fig. 23 delayed vortex breakdown whereas a similar increase in Fig. 22 had the opposite effect. On the other hand, for b/w = 0.7 the vortex breakdown is delayed (Fig. 23), particularly at higher angles of attack, in contrast to the data for b/w = 0.68 in the water tunnel (Fig. 22), which did not display the same breakdown delay at high alpha. This indicates that additional parameters are at play. It is likely that the longitudinal static pressure gradient near the tunnel wall could have had a significant effect on vortex breakdown for the large model (b/w = 0.7) in Fig. 23. At low alpha the adverse longitudinal pressure gradient due to the presence of the support will promote vortex breakdown to some extent. However, with increasing alpha the increasing wake blockage of the delta wing produces a dynamic pressure increment with associated favorable static pressure gradient in the outer region [57]. It has been shown in unsteady tests of aircraft models that this effect increases rapidly for relative model sizes b/w > 0.5 (Ref. 57). In the case of b/w = 0.7 in Fig. 23 this effect appears to have delayed vortex breakdown substantially.

Whereas the differences in Reynolds number, support geometries, and the presence/absence of a mounting body are likely to have played a role, there are other factors which should also be considered. It should be noted that the nature of wall interference in a horizontal-circuit water tunnel is different from that in the wind tunnel owing to the presence of a free surface. For large blockage ratios the test section flow is distorted by turbulence due to surface gravitational action and the dynamic pressure increment is opposite to that for solid walls. Consequently, if the tests were performed with the apex pointing downwards, the vortex breakdown would not be expected to be delayed significantly for the large model at high angles of attack, in agreement with the experimental results in Fig. 22. If the apex had been pointing upwards, vortex breakdown would have been delayed at high alpha, just as in the wind tunnel test [43] (Fig. 23). With the apex pointing downward the wall-induced positive camber would be similar in the water tunnel and the wind tunnel, suggesting that in the former case the adverse pressure gradients due to the overhead support structure were dominant at low alpha. This is not surprising because in that case the local wake blockage is upstream of the strut, exacerbating the free surface effect. The difference in test Reynolds number for the two models could also have played a role.

The test engineer's dilemma when trying to investigate the effect of Reynolds number on delta-wing vortex breakdown in a standard wind tunnel facility is well illustrated by the experimental results in Figs. 22, 23, and 28. The experimental results in Fig. 23 can be used to illustrate the problem encountered when investigating the effect of leading-edge sweep, while keeping the delta-wing chord constant in order to keep the Reynolds number constant. In that case the ratio b/w will vary with the sweep angle Λ as follows

$$b/w = (2c/w) \cot \Lambda \qquad (2)$$

Equation (2) shows that if b/w = 0.175 for $\Lambda = 80^o$, decreasing the sweep to $\Lambda = 70^o$ and $\Lambda = 60^o$ would result in b/w = 0.260 and b/w = 0.575, respectively. The results in Fig. 23 indicate that these b/w values would prevent the test from showing the true effect of leading-edge sweep. Although it is undeniably true that both support interference and wind tunnel wall interference can in many cases severely distort the experimental results, it should be emphasized that a test engineer that is knowledgeable about

these difficulties can select model size and test parameters that will bring these ground facility interference effects down to tolerable magnitudes.

Although much of the discussion here has been focused on the effect of ground facility interference on the static vortex breakdown characteristics, it should be pointed out, as is done in Ref. 39, that the interference effect becomes of even greater concern for a delta wing describing pitching or rolling motions.

3 Conclusions

Analysis of published experimental results for delta wing models leads to the conclusion that in subscale tests of wings with highly swept leading edges the concerns of Reynolds number scaling, wind tunnel wall interference, and model support interference place conflicting requirements on the test parameters which need to be considered in the early planning stages to assure the quality of the test results.

A large step toward achieving the needed simulation capability is to minimize and possibly eliminate support interference effects, using available new technologies [18] capable of generating sufficiently low support interference. At the same time the intrusive nature of conventional testing techniques has to be recognized, exemplified by the disturbances caused by the instrumentation used for pressure measurements as well as by the orifices used for dye flow visualization.

Further prequisites for minimizing the aerodynamic distortion at high angles of attack include the appropriate choice of sting/balance housing geometry, and judicious application of boundary layer trips or roughness in low Reynolds number tests.

The ultimate problem, i.e., to simulate full-scale Reynolds number flow conditions in subscale model tests, can only be solved if the viscous flow interactions at moderate angles of attack associated with small-scale geometric features are understood better.

References

[1] Scott, W. B., “Better modeling will alter culture of flight testing,” Aviation Week & Space Technology, March 23, 1998, pp. 84-86.

[2] Fulghum, D. A., “U. S. industry searches for design formulas,” Aviation Week & Space Technology, June 2, 1997, pp. 49, 50.

[3] Fulghum, D. A., “Payload, not airframe drives UCAV research,” Aviation Week & Space Technology, June 2, 1997, pp. 51-54.

[4] Fulghum, D. A., “ Unmanned strikenNext for military,” Aviation Week & Space Technology, June 2, 1997, pp. 47, 48.

[5] Hummel, D., “ Experimentelle Untersuchung der Strömung auf der Saugseite eines schlanken Deltaflügels,” Zeitschrift für Flugwissenschaften, 13 (1965), Heft 7, pp. 249-252.

[6] Ericsson, L. E., “Effect of pitch rate on delta wing vortex characteristics,” AIAA Paper 96-3405, July 1996.

[7] Ericsson, L. E., “Pitch rate effects on delta wing vortex breakdown,” Journal of Aircraft, Vol. 33, No. 3, 1996, pp. 639-642.

[8] Lambourne, N. C., Bryer, D.W., and Maybrey, J. F. M., “Pressure measurements on a model delta wing undergoing oscillatory deformation,” NPL Aero Report 1314, March 1970, Aeronautical Research Council, Great Britain.

[9] Ericsson, L. E. and Reding, J. P., “Fluid mechanics of dynamic stall, part II, Prediction of full scale characteristics,” Journal of Fluids and Structures, Vol. 2, March 1990, pp. 113-143.

[10] Ericsson, L. E., “Transition effects on airfoil dynamics and the implication for subscale tests,” Journal of Aircraft, Vol. 26, No. 12, 1989, pp. 121-144.

[11] Ericsson, L. E., “Effect of transition on wind tunnel simulation of vehicle dynamics,” Progress of Aerospace Sciences, Vol. 27, 1990, pp. 121-144.

[12] Ericsson, L. E. and Hanff, E, S., “Further analysis of high-rate rolling experiments of a 65-deg delta wing,” Journal of Aircraft, Vol. 3, No. 6, 1994, pp. 1350-1357.

[13] Hanff, E. S. and Jenkins, S. B., “Large-amplitude high-rate roll experiments on a delta and double-delta wing,” AIAA Paper 90-0224, Jan. 1990.

[14] Ericsson, L. E., “Effect of fuselage geometry on delta wing vortex breakdown,” Journal of Aircraft, Vol. 35, No. 6, 1998, pp. 898-904.

[15] Ericsson, L. E., “Review of transition effects on the problem of dynamic simulation,” AIAA Paper 88-2004, May 1988.

[16] Krogmann, P., "Experimentelle und theoretische Untersuchungen an Doppeldelta Flügeln," Aerodynamische Versuchsanstalt, Göttingen FRG, Bericht 68A35, July 1968.

[17] Skow, A. M., Comment in Round Table Discussion, AGARD-CP-247, 1978, p. RTD-4.

[18] Beyers, M. E. and Ericsson, L. E., "Aerodynamic simulation difficulties in subscale tests of combat aircraft," AIAA Paper 99-0683, Jan. 1999.

[19] Jobe, C. E., "Vortex breakdown location over 65^o delta wings-empiricism and experiment", AIAA Paper 98-2526-CP, June 1998.

[20] Ericsson, L. E., "Explanation for huge differences between measurements of vortex breakdown on 65 deg delta-wing configurations," AIAA Paper 99-4100, Aug. 1999.

[21] Huang, X. Z. and Hanff, E. S., "Unsteady behavior of spiral vortex breakdown," AIAA Paper 96-3408-CP, July 1996.

[22] Huang, X. Z., Sun, Y. Z., and Hanff, E. S., "Circulation criterion to predict leading-edge vortex breakdown over delta wings," AIAA Paper 97-2265, June 1997.

[23] Pelletier, A. and Nelson, R. C., "An experimental study of static and dynamic vortex breakdown on slender delta wing planforms," AIAA Paper 94-1879-CP, June 1994.

[24] Addington, G. A., "The role of flow field structure in determining the aerodynamicrResponse of a delta wing," Ph. D. Dissertation, University of Notre Dame, Notre Dame, IN, April 1998.

[25] Cipolla, K. M., "Structure of the flow past delta wing with variations in roll angle," Ph. D. Dissertation, Lehigh University, May 1996.

[26] Huang, X. Z., Sun, Y. Z., and Hanff, E. S., "Further investigation of leading-edge vortex breakdown over delta wings," AIAA Paper 97-2263-CP, June 1997.

[27] Lowson, M. V. and Riley, A. J., "Vortex breakdown control by delta wing geometry," Journal of Aircraft, Vol. 32, No. 4, 1995, pp. 832-838.

[28] Lambourne, N. C. and Bryer, D. W., "The bursting of leading-edge vortices--some observations and discussion of the phenomenon," Aeronautical Research Council, R&M 3282, Great Britain, April 1961.

[29] Wentz, W. H. and Kohlman, D. L., "Vortex breakdown on slender sharp-edged delta wings," Journal of Aircraft, Vol. 8, No. 3, 1971, pp. 156-161.

[30] Ericsson, L. E. and King, H. H. C., "Effect of cross-sectional geometry on slender delta wing unsteady aerodynamics," Journal of Aircraft, Vol. 30, No. 5, 1993, pp. 793-795.

[31] Guglieri, G. and Quagliotti, F. B., "Experimental investigation of vortex dynamics on delta wings," AIAA Paper 92-2731-CP, June 1992.

[32] Verhagen, N. G., "Effect of sideslip on the flow over a 65-deg delta wing; Preliminary report," Delft University of Technology, The Netherlands, Dec. 1997.

[33] Gursul, I., "Unsteady flow phenomena over delta wings," AIAA Journal, Vol. 32, No. 2, 1994, pp. 225-231.

[34] Fritzelas, A. E., Platzer, M. F., and Hebbar, S. K., "Effect of Reynolds number on high-incidence flow over double-delta wings," AIAA Paper 97-0046, Jan. 1997.

[35] Ericsson, L. E., "Further analysis of fuselage effects on delta wing aerodynamics," AIAA Paper 2000-0981, Jan. 2000.

[36] Panton, R. L., "Effects of a contoured apex on vortex breakdown," Journal of Aircraft, Vol. 27, No. 3, 1990, pp. 285-288.

[37] Straka, W. A. and Hemsch, M. J., "Effect of fuselage on delta wing vortex breakdown," Journal of Aircraft, Vol. 31, No. 4, 1994, pp. 1002-1005.

[38] Ericsson, L. E., "Effect of fuselage on delta wing vortex breakdown," Journal of Aircraft, Vol. 31, No. 4, 1994, pp. 1006-1007.

[39] Ericsson, L. E. and Beyers, M. E., "Ground facility interference on slender vehicle unsteady aerodynamics," Journal of Aircraft, Vol. 33, No. 1, 1996, pp. 117-124.

[40] Ericsson, L. E. and Beyers, M. E., "Wind tunnel aerodynamics in rotary tests of combat aircraft models," Journal of Aircraft, Vol. 35, No. 4, 1996, pp. 521-528.

[41] Pelletier, A. and Nelson, R. C., "Factors influencing vortex breakdown over 70^o delta wings," AIAA Paper 95-3469-CP, Aug. 1995.

[42] Ericsson, L. E. and Beyers, M. E., "Aspects of ground facility interference on leading-edge vortex breakdown," AIAA Paper 2000-0978, Jan. 2000.

[43] Weinberg, Z., "Effect of tunnel walls on vortex breakdown location over delta wings," AIAA Journal, Vol. 30, No. 6, 1992, pp. 1584-1586.

[44] Ericsson, L. E. and Reding, J. P., "Unsteady aerodynamics of slender delta wings at large angles of attack," Journal of Aircraft, Vol. 12, No. 9, 1975, pp. 721-729.

[45] Polhamus, E.C., "A concept of the vortex lift of sharp-edged delta wings based on a leading-edge-suction analogy," Journal of Aircraft, Vol. 8, No. 4, 1971, pp. 193-199.

[46] Ericsson, L. E. and Reding, J. P., "Approximate nonlinear slender wing aerodynamics," Journal of Aircraft, Vol. 14, No. 12, 1977, pp. 1192-1204.

[47] Ericsson, L. E. and King, H. H. C., "Rapid prediction of high-alpha unsteady aerodynamics of slender wing aircraft," Journal of Aircraft, Vol. 29, No. 1, 1992, pp. 85-92.

[48] Ericsson, L. E., “Dynamic stall of pitching airfoils and slender wings -- similarities and differences,”. Journal of Aircraft, Vol. 36, No. 3, 1999, pp. 603-605.

[49] Soltani, M. R. and Bragg, M. B., “Early vortex burst on a delta wing inpPitch,” AIAA Journal, Vol. 31, No. 12, 1993, pp. 1283-1289.

[50] Beyers, M. E. and Ericsson, L. E., “Ground facility interference on aircraft configurations with separated flow,” Journal of Aircraft, Vol. 30, No. 5, 1993, pp. 682-688.

[51] Ericsson, L. E. and Reding, J. P., “Dynamic support interference in high alpha testing,” Journal of Aircraft, Vol. 23, No. 12, 1986, pp. 889-896.

[52] Ericsson, L. E., “Another look at high-alpha support interference in rotary tests,” Journal of Aircraft, Vol. 28, No. 9, 1991, pp. 584-591.

[53] Hummel, D., “Untersuchung über das Aufplatzen der Wirbel an Deltaflügeln,” Zeitschrift für Flugwissenschaften und Weltraumforschung, Vol. 5, No. 6, 1981, pp. 349-366.

[54] Wenhua, Z., Kewen, D., Da, H., Zuigiang, L., and Quingli, Z., “Tunnel interference in unsteady post stall experiments,” Chinese Journal of Aeronautics, Vol. 10, No. 4, 1997, pp. 247-254.

[55] Pamadi, B. N., Rao, D. M., and Niranjana, T., “Roll attractor of delta wings at high angles of attack,” International Council of the Aeronautical Sciences, 94-7.1.2, Sept. 1994.

[56] Ericsson, L. E., “Analysis of the effect of sideslip on delta wing roll-trim characteristics,” Journal of Aircraft, Vol. 34, No. 5, 1997, pp. 585-591.

[57] Beyers, M. E., “Unsteady wind tunnel interference in aircraft dynamic experiments,” Journal of Aircraft, Vol. 29, No. 6, 1992, pp. 1122-1129.